Rock Mech. Rock Engng. (2008) 41 (5), 715–734
DOI 10.1007/s00603-007-0146-7
Printed in The Netherlands

Rock Mechanics
and Rock Engineering

Efficient Probabilistic Algorithm Illustrated for a Rock Slope

By

B. K. Low

School of Civil and Environmental Engineering, Nanyang Technological University, Singapore

Received March 16, 2007; accepted May 16, 2007
Published online September 18, 2007

Summary

A new spreadsheet-based algorithm for the first-order reliability method (FORM) is illustrated for a two-dimensional rock slope of Hong Kong. The new algorithm combines inverse distribution functions and a refined Newton method with the automatic constrained-optimization search of the design point in the original space of the random variables; it obviates the need for computations of equivalent normal means and equivalent normal standard deviations. In the rock slope analysis, the versatile 4-parameter beta distribution is used in lieu of a truncated normal distribution. Probabilities of failure inferred from reliability indices are compared with those from Monte Carlo simulations. The effects of parametric correlations on the required reinforcing force for a target reliability index value are studied. The intuitive perspective of an expanding equivalent dispersion ellipsoid in the original space of the basic random variables is also described as it is the basis from which the new approach evolved.

Keywords: Rock slope, reliability, FORM, Monte Carlo, constrained optimization, spreadsheet.

1. Introduction

The conventional factor of safety in geotechnical engineering cannot reflect the uncertainty of its underlying parameters. A more rational approach is to evaluate a reliability index β that depends not only on the mean values of the parameters but also on their scatter and correlations. Among the various definitions of reliability indices, the Hasofer-Lind (1974) index for normal random variables and the first-order reliability method (FORM) for nonnormal random variables are more consistent and rigorous, but – as traditionally presented – also more mathematical. These conceptual and implementation barriers can largely be overcome, by adopting the alternative perspective of an expanding equivalent dispersion ellipsoid in the original space of the variables, and using an optimization routine available in the Microsoft Excel spreadsheet

software, as described in Low and Tang (1997a, 2004) and further illustrated in Low (2005). Correlated nonnormal random variables can be viewed as forming a tilted equivalent ellipsoid in the original space of the random variables, centered not at the original mean values of the nonnormal variates but at their equivalent normal means. There is no need to diagonalize (tantamount to rotating the frame of reference) the covariance or correlation matrix.

This paper aims to further reduce the computational and conceptual barriers of the first-order reliability method (FORM) for correlated nonnormals, using the Sau Mau Ping rock slope of Hong Kong as an illustration. The new spreadsheet-based practical algorithm presented herein is an alternative to the Low and Tang 1997 and 2004 approaches. Unlike the earlier approaches, the new algorithm obviates the need for computations of the means and standard deviations of equivalent normal distributions, and varies (automatically during constrained optimization) a set of *dimensionless* numbers rather than the basic random variables with its miscellaneous units. The Sau Mau Ping rock slope was analyzed in Low (2007) using the Low and Tang (2004) approach. The random variables were modelled using the normal and the truncated exponential distributions. In this study the same slope is revisited, and analyzed using the Low and Tang (2007) new algorithm and different probability distributions.

Some concepts pertaining to the reliability index are presented next. Subsequent sections will present the application of the new probabilistic algorithm to the rock slope in Hong Kong, in which the random variables are modeled by truncated exponential distributions and the versatile 4-parameter beta distributions. The effects of correlations on the required reinforcing force for a desired reliability index are studied. Comparisons are made with Monte Carlo simulations. It will be shown that the new algorithm is particularly convenient with respect to its choice of the initial point prior to constrained optimization, and when there is a need to test the robustness of the search through randomization of initial points.

The emphasis of the new algorithm in this study is on obtaining the FORM solution with efficiency, understanding, intuitive appreciation, and relative transparency.

2. Perspective of Expanding Equivalent Dispersion Ellipsoid for Normals and Nonnormals

The Hasofer-Lind (1974) index for cases with correlated normal random variables and the first-order reliability method (FORM) for cases with correlated nonnormals are well explained in Ditlevsen (1981), Shinozuka (1983), Ang and Tang (1984), Melchers (1999), Haldar and Mahadevan (1999), and Baecher and Christian (2003), for example. The potential inadequacies of the FORM in some cases have been recognized, and more refined alternatives proposed, in Chen and Lind (1983), Der Kiureghian et al. (1987), Wu and Wirsching (1987), and Zhao and Ono (2001), among others. On the other hand, the usefulness and accuracy of the FORM in most applications are well recognized, for instance in Rackwitz (2001). The focus of this paper is on the FORM, which includes the Hasofer-Lind index as a special case.

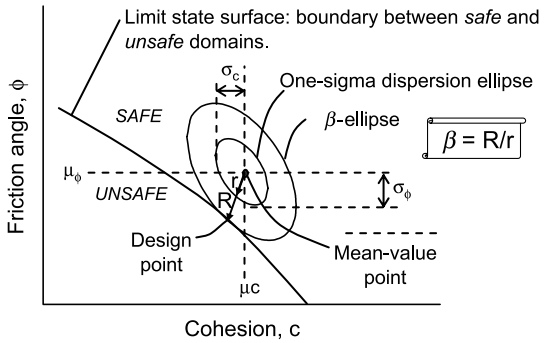

Fig. 1. Illustration of the reliability index β in the plane. The symbols μ and σ denote the mean value and the standard deviation, respectively

Low and Tang (1997a) presented a practical and transparent FORM procedure using spreadsheet-automated constrained optimization based on the perspective of an expanding equivalent dispersion ellipsoid in the original space of the basic random variables (Fig. 1). The Rackwitz-Fiessler (1978) equivalent normal transformation was used, but the concepts of coordinate transformation and frame-of-reference rotation were not required. Correlation was accounted for by setting up the quadratic form directly. Iterative searching and partial derivatives were automatic. This spreadsheet-cell-object-oriented constrained optimization approach was subsequently extended in Low and Tang (2004), by testing robustness and accuracy for various nonnormal distributions and more complicated performance functions, and by providing enhanced operational convenience and versatility.

The matrix formulation (Veneziano 1974, Ditlevsen 1981) of the Hasofer-Lind (1974) index β is:

$$\beta = \min_{\underline{x} \in F} \sqrt{(\underline{x} - \underline{\mu})^T \underline{C}^{-1} (\underline{x} - \underline{\mu})} \tag{1a}$$

or, equivalently:

$$\beta = \min_{\underline{x} \in F} \sqrt{\left[\frac{x_i - \mu_i}{\sigma_i}\right]^T [\underline{R}]^{-1} \left[\frac{x_i - \mu_i}{\sigma_i}\right]} \tag{1b}$$

where $\underline{x}$ is a vector representing the set of random variables x_i, $\underline{\mu}$ the vector of mean values μ_i, $\underline{C}$ the covariance matrix, $\underline{R}$ the correlation matrix, σ_i the standard deviation, and F the failure domain. Low and Tang (1997b and later) used Eq. (1b) in preference to Eq. (1a) because the correlation matrix $\underline{R}$ is easier to set up, and conveys the correlation structure more explicitly than the covariance matrix $\underline{C}$.

The point denoted by the x_i values which minimize Eq. (1) and satisfies $\underline{x} \in F$ is the design point – the point of tangency of an expanding dispersion ellipsoid with the limit state surface which separates safe combinations of parametric values from unsafe combinations (Fig. 1). For correlated normals, one may note that the quadratic form in

Eq. (1a) appears also in the negative exponent of the established probability density function of the multivariate normal distribution:

$$f(\underline{x}) = \frac{1}{(2\pi)^{\frac{n}{2}}|C|^{0.5}} \exp\left[-\frac{1}{2}(\underline{x} - \underline{\mu})^T C^{-1} (\underline{x} - \underline{\mu}) \right] \tag{2a}$$

$$= \frac{1}{(2\pi)^{\frac{n}{2}}|C|^{0.5}} \exp\left[-\frac{1}{2}\beta^2 \right] \tag{2b}$$

where β is defined by Eq. (1a) or (1b), without the ''min''. As a multivariate normal dispersion ellipsoid expands from the mean-value point, its expanding surfaces are contours of decreasing probability values. Hence, to obtain β by Eq. (1) means maximizing the value of the multivariate normal probability density function (Eq. (2)), and is graphically equivalent to finding the smallest ellipsoid tangent to the limit state surface at the most probable failure point (the *design point*). This intuitive and visual understanding of the *design point* is consistent with the more mathematical approach in Shinozuka (1983), in which all variables were standardized and the limit state equation was written in terms of standardized variables.

For correlated nonnormals, the ellipsoid perspective still apply in the original coordinate system, except that the nonnormal distributions are replaced by an equivalent normal ellipsoid, centered not at the original mean values of the nonnormal distributions, but at the equivalent normal mean $\underline{\mu}^N$:

$$\beta = \min_{\underline{x} \in F} \sqrt{[x_i - \mu_i^N]^T [\underline{C}^N]^{-1} [x_i - \mu_i^N]} \tag{3a}$$

or, equivalently, in terms of correlation matrix R,

$$\beta = \min_{\underline{x} \in F} \sqrt{\left[\frac{x_i - \mu_i^N}{\sigma_i^N} \right]^T [\underline{R}]^{-1} \left[\frac{x_i - \mu_i^N}{\sigma_i^N} \right]} \tag{3b}$$

In Eq. (3a), $\underline{C}^N$ is covariance matrix based on the equivalent normal standard deviation $\underline{\sigma}^N$. The values of μ_i^N and σ_i^N in both equations can be obtained by equating the cumulative probability as well as the probability density ordinate of the equivalent normal distribution to those of the corresponding nonnormal distribution at the point x, resulting in the following Rackwitz-Fiessler (1978) two-parameter equivalent normal distribution:

Equivalent normal standard deviation:

$$\sigma^N = \frac{\phi\{\Phi^{-1}[F(x)]\}}{f(x)} \tag{4}$$

Equivalent normal mean:

$$\mu^N = x - \sigma^N \times \Phi^{-1}[F(x)] \tag{5}$$

where x is the original nonnormal variate, $\Phi^{-1}[\cdot]$ is the inverse of the standard normal cumulative distribution (CDF), $F(x)$ is the original nonnormal CDF evaluated at x, $\phi\{\cdot\}$ is the probability density function (pdf) of the standard normal distribution, and $f(x)$ is the original nonnormal probability density ordinate at x.

The next two sections compare the reliability analyses of a Hong Kong slope based on the two different spreadsheet algorithms of Low and Tang (2004, 2007), respectively.

3. Rock Slope Analyzed using 2004 Algorithm for the FORM via Varying Basic Random Variables x_i

The spreadsheet FORM procedure of this section was described in Low and Tang (1997a, b, 2004), using Eqs. (3a), (1b) and (3b), respectively. It is the basis from

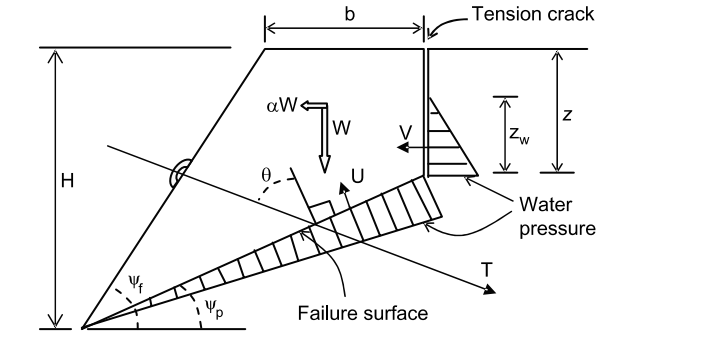

Plane sliding formulation and data of Sau Mau Ping slope (Ref. Hoek 2006)

$$F_s = \frac{cA + N' \tan\phi}{W(\sin\psi_p + \alpha\cos\psi_p) + V\cos\psi_p - T\sin\theta}$$

where $A = (H - z)/\sin\psi_p$

$$N' = W(\cos\psi_p - \alpha\sin\psi_p) - U - V\sin\psi_p + T\cos\theta$$

$$W = 0.5\gamma H^2\left(\left(1 - \left(\frac{z}{H}\right)^2\right)\cot\psi_p - \cot\psi_f\right)$$

$$U = 0.5\gamma_w z_w A \qquad V = 0.5\gamma_w z_w^{\ 2}$$

$$b = (H - z)\cot\psi_p - H\cot\psi_f \qquad z = H - (b + H\cot\psi_f)\tan\psi_p$$

For Sau Mau Ping slope of Hong Kong

Deterministic parameters: H = 60 m, ψ_f = 50°, ψ_p = 35°, T = 0,
γ = 2.6 tonne/m^3, γw = 2.6 tonne/m^3.

Random variable	Distribution	Mean μ	Standard deviation
c	Normal	10 t/m^2	2 t/m^2
ϕ	Normal	35°	5°
b	Normal	15.3 m	4.2 m
z_w	Exponential, μ = 0.5z, truncated to (0, z)		
α	Exponential with mean 0.08, truncated to (0, 0.16)		

α = Ratio of horizontal earthquake acceleration to gravitational acceleration

Fig. 2. Analytical model and data of the Sau Mau Ping slope

which the new alternative procedure of the next section evolved. Both procedures will be illustrated in the context of the Sau Mau Ping slope of Hong Kong (Fig. 2).

Hoek (2006) used the horizontal distance b of the tension crack behind the slope crest as input in place of the tension crack depth z because b can be measured in the field and also because it is not influenced by the inclination of the upper slope. Statistical data for z was given as $\mu = 14$ m and $\sigma = 3$ m, and for b as $\mu = 15.3$ m and $\sigma = 4.2$ m. These two sets of data are consistent because b and z are geometrically related by the two equations of b and z shown in Fig. 2 and, for the given H, ψ_p, ψ_f, reduces to $b = 35.3 - 1.43\,z$, from which the μ and σ of b are obtained when those of z are known. Because z and b are geometrically related, either can be treated as a random variable, but not both. The reliability analyses of this and the next sections consider b as random, as did Hoek (2006) in his Monte Carlo simulations.

Figure 3 obtains the reliability index for Sau Mau Ping slope based on Eqs. (3b), (4) and (5). It invokes a user-created Microsoft Excel VBA function *EqvN*, described

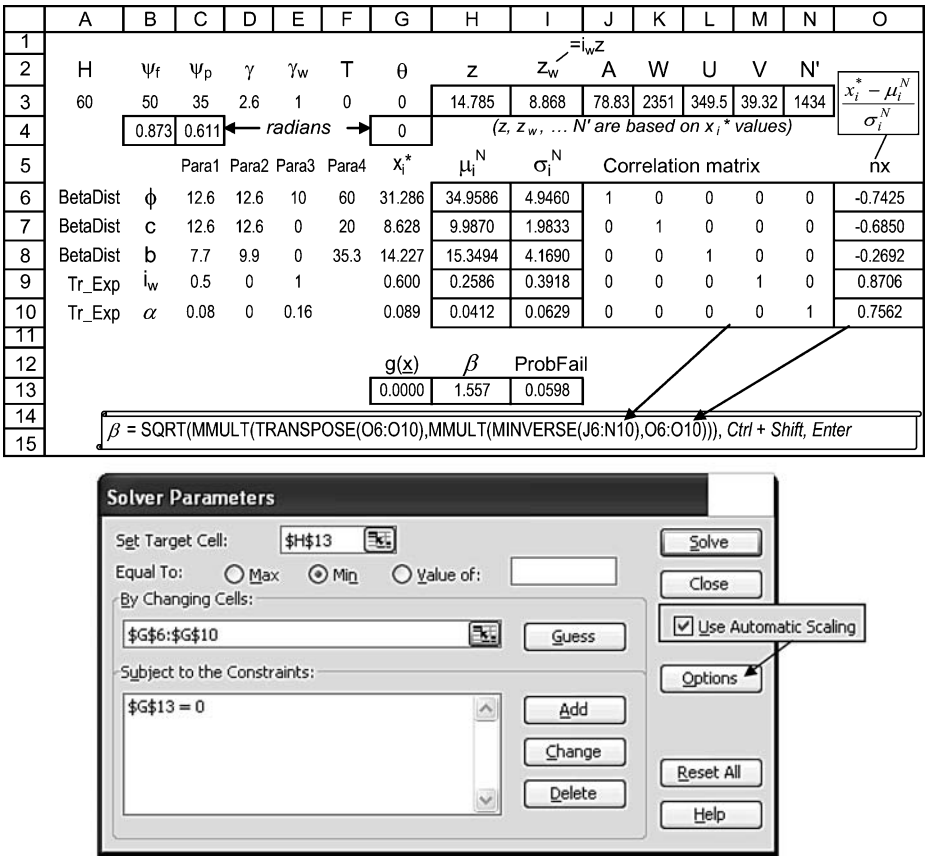

Fig. 3. First-order reliability method (FORM) for the Sau Mau Ping slope, using the Low and Tang (2004) algorithm. Initially the x_i^* column values were (35, 10, 15.3, 0.5, 0.08)

in Low and Tang (2004), to compute the equivalent normal μ_i^N and σ_i^N by Eqs. (4) and (5) for various nonnormal distributions. This approach results in a clear and convenient user interface where various nonnormal distributions can be selected at ease without the need to modify the template for different probability distributions. The key feature was that distribution-specific equations were relegated to a short program code (created inside Microsoft Excel) which was called by cells beneath the headings μ_i^N and σ_i^N in Fig. 3. (An Excel file of the Low and Tang (2004) procedure, with performance function $g(\underline{X}) = YZ - M$, can be downloaded from http://alum.mit.edu/www/bklow, for better understanding by doing this hands-on.)

Instead of the truncated normal distributions used in Hoek (2006), Fig. 3 uses the 4-parameter bounded beta distributions for ϕ, c and b, with bounded range (10, 60), (0, 20) and (0, 35.3), respectively. The versatility of the 4-parameter beta distribution is illustrated in Fig. 4 for a random variable with a bounded range (0, 1). In the beta distribution with parameters a_1, a_2, min and max, the third and fourth parameters define the lower and upper limits of the range, while the first two parameters are shape parameters. If $a_1 = a_2$, the beta distribution curve is non-skew, as shown by the curves labeled (2, 2, 0, 1), (3, 3, 0, 1), (5, 5, 0, 1) and (9, 9, 0, 1). Also, the curves labeled (1.5, 4, 0, 1) and (4, 1.5, 0, 1) exhibit symmetry.

Comparisons between the normal distributions and the bounded beta distributions of ϕ, c and b, and between the truncated exponential distribution (of i_w and α) and a

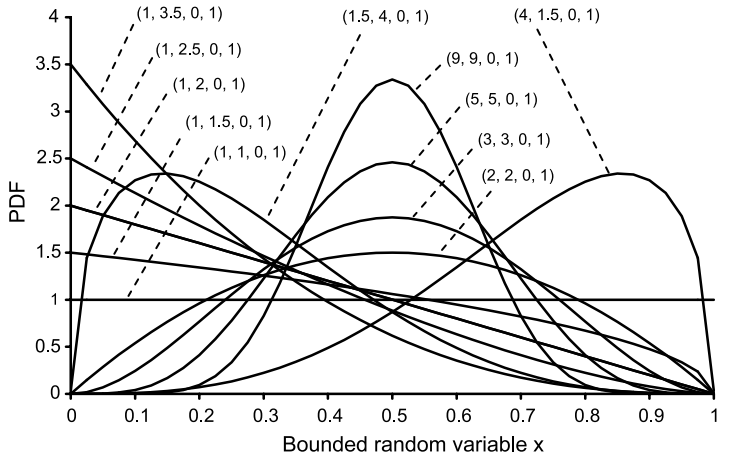


```
The beta PDF curves can be plotted using the following user-defined function in Excel:
Function Betapdf(x, a1, a2, min, max)
 With Application.worksheet function
  BetaFunc = Exp(.GammaLn(a1) + .GammaLn(a2) - .GammaLn(a1 + a2))
  Betapdf = 1 / BetaFunc * (x - min) ^ (a1 - 1) * (max - x) ^ (a2 - 1) / (max - min) ^ (a1 + a2 - 1)
 End With
End Function
```

Fig. 4. Versatility of the 4-parameter general beta distribution; the first 2 parameters are shape parameters, the last two parameters define the range

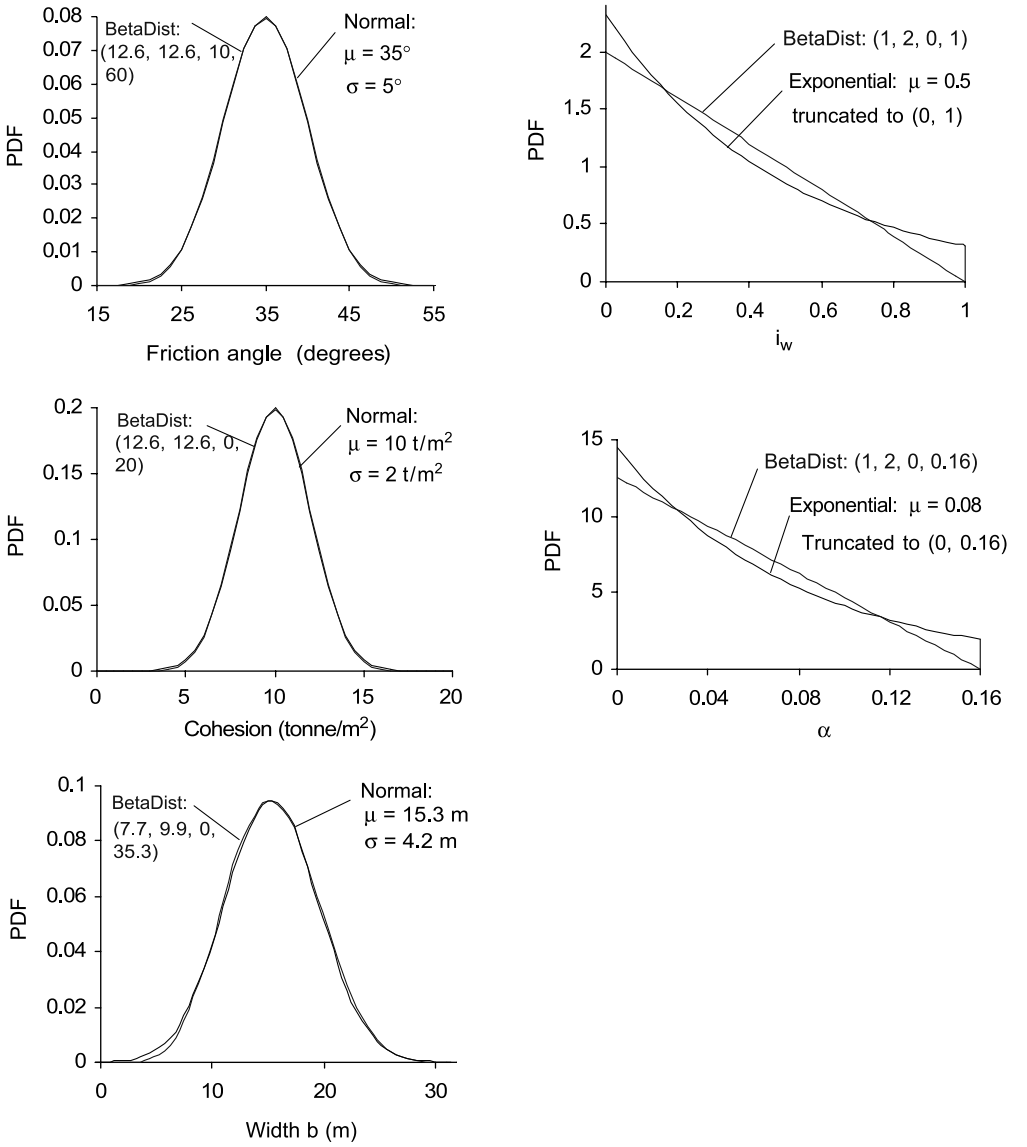

Fig. 5. General beta distributions for ϕ, c and b, in lieu of truncated normals, and exponentials of i_w $(= z_w/z)$ and α, the latter with original mean values 0.5 and 0.08, truncated to (0, 1) and (0, 0.16), respectively

special triangular form of the beta distribution, are shown in Fig. 5. It can be seen from the PDF curves of ϕ and cohesion that the beta distribution with the four parameters $a_1 = 12.6$, $a_2 = 12.6$, $\min = \mu - 5\sigma$ and $\max = \mu + 5\sigma$ are very good approximations of the Normal distribution $N(\mu, \sigma)$, and has advantage over the latter in being bounded. The PDF of width b is asymmetrical because its mean (15.3 m) is not at the centre of its range (0, 35.3).

The performance function (cell G13, Fig. 3) is based on the following entered equations:

$$g(x) = cA + N' \tan\phi - [W(\sin\psi_p + \alpha\cos\psi_p) + V\cos\psi_p - T\sin\theta] \tag{6}$$

where the symbols are as defined in Fig. 2. One can also define $g(x) = F_s(c, \phi, \ldots) - 1$, which is equivalent to Eq. (6) when $g(x)$ is constrained to be zero during Solver optimization.

The equation for N′ (cell N3, Fig. 3) is entered as follows:

$$N' = \max(0, W(\cos\psi_p - \alpha\sin\psi_p) - U - V\sin\psi_p + T\cos\theta) \tag{7}$$

This constrains N′ to be $\geqslant 0$ (i.e., non-negative), consistent with physical considerations.

The square root of the quadratic form in Eq. (3b) was computed directly as β in cell H13 using the array formula:

$$\text{`` } = \text{sqrt(mmult(transpose}(nx),\ \text{mmult(minverse(crmat)}, nx))) \text{''} \tag{8}$$

in which *mmult*, *transpose* and *minverse* are Excel's built-in functions, each being a container of program codes for matrix operations. The *nx* vector in cells O6:O10 contain equations $(x_i - \mu_i^N)/\sigma_i^N$.

The design point (x^* values) was obtained by using Microsoft Excel's built-in optimization routine Solver, to minimize the β cell, by changing the x^* values, subject to the constraint that the performance function $g(x) = 0$. Prior to the Excel Solver search, the x^* values had values equal to the mean values (35, 10, 15.3, 0.5, 0.08) of the original random variables. Iterative numerical derivatives and directional search for the design point x^* were automatic.

From the computed reliability index β of 1.557 in Fig. 3, the probability of failure can be estimated from $P_f \approx \Phi(-\beta)$, where $\Phi(\cdot)$ is the standard normal cumulative distribution. For this, the equation `` = NormSDist(-H13)'' was entered in cell I13, yielding a P_f value of about 6.00%.

Five Monte Carlo simulations each with 50,000 trials were carried out using the specialized software @RISK (http://www.palisade.com), based on the original nonnormal distributions (beta and truncated exponential distributions). The probabilities of failure $(g(x) < 0)$ were 6.12, 6.28, 6.15, 6.11, 6.29%, respectively, averaging 6.19%. A separate run with 200,000 trials yielded 6.15%, taking 56 sec. Another run with 200,000 trials yielded 6.24%. For comparison, the $P_f = 5.98\%$ (from reliability index $\beta = 1.557$) in Fig. 3 were obtained using the Low and Tang (2004) procedure in about 2 sec.

(If desired, the original correlation matrix (ρ_{ij}) of the nonnormals can be modified to ρ'_{ij} in line with the equivalent normal transformation, as suggested in Der Kiureghian and Liu (1986). Some tables of the ratio ρ'_{ij}/ρ_{ij} are available in Melchers (1999), including the closed form solution for the special case of lognormals. For simplicity, the examples of this study retain the original unmodified correlation matrices.)

4. Rock Slope Analyzed using the Alternative Algorithm for the FORM via Varying Dimensionless Numbers n_i

In Fig. 3, the x_i values (cells G6:G10) were changed during the constrained optimization. The n_x column (cells O6:O10) contain equations to compute $(x^* - \mu^N)/\sigma^N$.

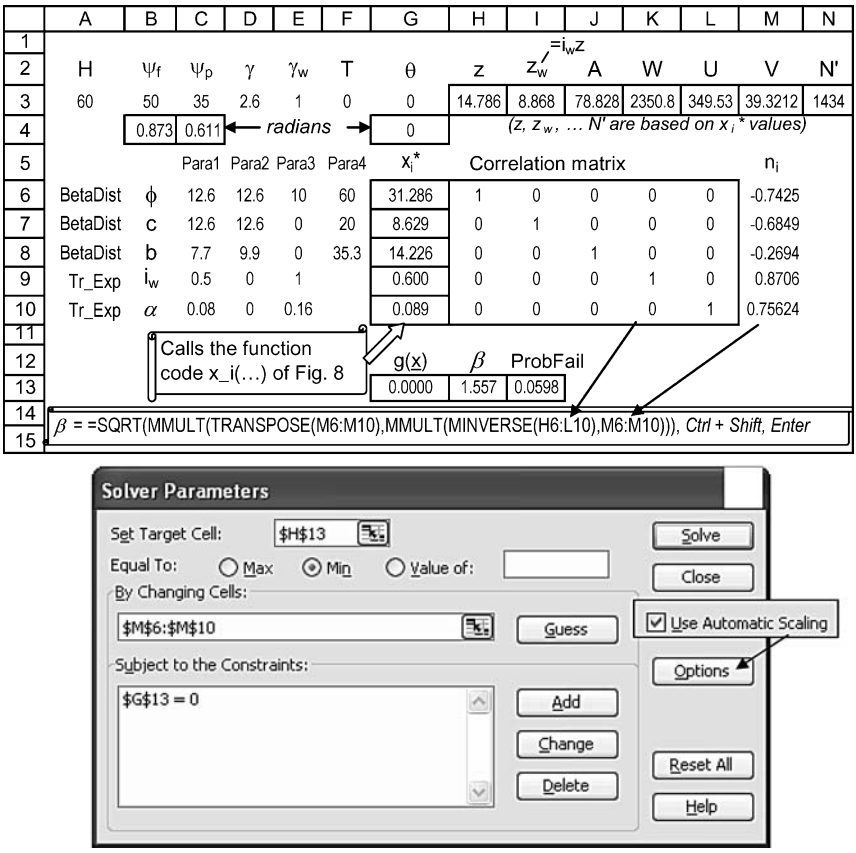

Fig. 6. Alternative first-order reliability method (FORM) for the Sau Mau Ping slope. Initially the n_i column values were zeros

In this section, a new approach is presented that varies the dimensionless numbers n_i (cells M6:M10, Fig. 6) during constrained optimization, and computes each x_i as a function of n_i. Equivalent normal means and equivalent normal standard deviations are not computed. This alternative approach has some advantages over that of Fig. 3.

The first and third terms under the square root sign in Eq. (3b) are the equivalent standard normal vector and, being functions of x_i, were denoted as nx in Fig. 3 (under column O). In the alternative approach of this section, the equivalent standard normal vector will be varied (automatically during Excel Solver's constrained optimization search) as numerical values (void of equations), hence n_i is used in Fig. 6 (to denote the cells M6:M10) instead of the nx of Fig. 3. Equation (3b) then becomes:

$$\beta = \min_{\underline{x} \in F} \sqrt{[\underline{n}]^T [\underline{R}]^{-1} [\underline{n}]} \tag{9}$$

where $\underline{n}$ is a column vector of dimensionless number n_i.

One notes that Eq. (5) can be rearranged a follows:

$$\frac{x_i - \mu_i^N}{\sigma_i^N} = \Phi^{-1}[F(x_i)] \tag{10}$$

However, in the approach of this section, the entity on the left side of Eq. (10) will be varied as a dimensionless number n_i (without computing the equivalent normal mean μ_i^N and the equivalent normal standard deviation σ_i^N), while the original random variable x_i will be computed as a function of n_i. Hence Eq. (10) is used in reverse, as follows:

$$\Phi(n_i) = F(x_i), \tag{11a}$$

i.e.,

$$x_i = F^{-1}[\Phi(n_i)] \tag{11b}$$

Equation (11b) renders it possible to back-calculate x_i for each trial value of n_i during Excel Solver's constrained optimization of Eq. (9). The objective is to find the value x_i such that the nonnormal cumulative probability distribution $F(x_i)$ at x_i is equal to the standard normal cumulative distribution $\Phi(n_i)$. The requirement that x_i be on the failure surface (limit state surface), $\underline{x} \in F$, is imposed as a constraint $g(\underline{x}) = 0$ in Excel Solver (Fig. 6). When this is satisfied and β by Eq. (9) is at its minimum, the $\underline{x}$ values become the design point $\underline{x}^*$ values.

The operational differences between the method of Fig. 3 and that of Fig. 6 are summarized in Fig. 7. The inverse distribution functions (Eq. (11b)) which enable x_i to be computed automatically as a function of n_i have been coded in Fig. 8. The closed form derivations are straightforward for normal, lognormal, truncated exponential, Gumbel, exponential, uniform, triangular and Weibull distributions. For example, for the truncated exponential distribution of mean a_1 and

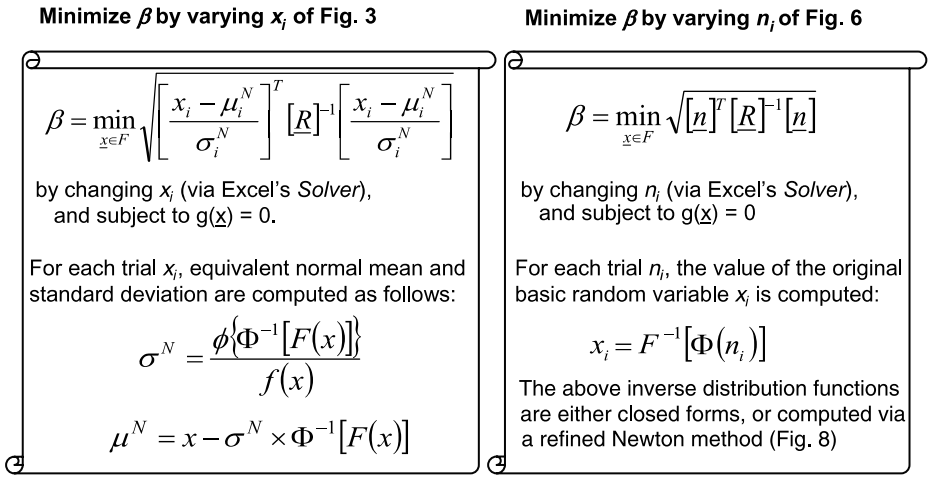

Fig. 7. Two methods compared: Fig. 3's method requires computation of equivalent normal means and equivalent normal standard deviations; Fig. 6's alternative method does not

```
Function x_i(DistributionName, para, ni) As Double
 a1 = para(1):  a2 = para(2):  a3 = para(3):  a4 = para(4)
 With Application.WorksheetFunction
 Select Case UCase(Trim(DistributionName))
  Case "NORMAL":     x_i = a1 + ni * a2
  Case "LOGNORMAL":  lamda = Log(a1) - 0.5 * Log(1 + (a2 / a1) ^ 2)
     zeta = Sqr(Log(1 + (a2 / a1) ^ 2)):  x_i = Exp(lamda + zeta * ni)
  Case "TR_EXP": lamda = 1 / a1:  tem = (Exp(-lamda * a2) - Exp(-lamda * a3))
   x_i = -a1 * Log(Exp(-lamda * a2) - tem * .NormSDist(ni))
  Case "EXTVALUE1":  alfa = 1.28255 / a2:  u = a1 - 0.5772 / alfa
   x_i = u - Log(-Log(.NormSDist(ni))) / alfa
  Case "EXPONENTIAL":  mean = a1:  x_i = -mean * Log(1 - .NormSDist(ni))
  Case "UNIFORM":    min = a1:  max = a2:    x_i = min + (max - min) * .NormSDist(ni)
  Case "TRIANGULAR":  a = a1:  m = a2:  c = a3:  tem = .NormSDist(ni):  maca = (m - a) / (c - a)
   If tem <= maca Then x_i = a + Sqr(tem * (m - a) * (c - a)) Else x_i = c - Sqr((1 - tem) * (c - a) * (c - m))
  Case "WEIBULL":    x_i = a2 * (-Log(1 - .NormSDist(ni))) ^ (1 / a1)
  Case "BETADIST":  min = a3:  max = a4:  xprev = min + (max - min) * a1 / (a1 + a2)
8: For k = 1 To 80
    CDF = .BetaDist(xprev, a1, a2, min, max)
    BetaFunc = Exp(.GammaLn(a1) + .GammaLn(a2) - .GammaLn(a1 + a2))
    pdf = 1 / BetaFunc * (xprev - min) ^ (a1 - 1) * (max - xprev) ^ (a2 - 1) / (max - min) ^ (a1 + a2 - 1)
    xnew = xprev - (CDF - .NormSDist(ni)) / pdf
    If Abs((xnew - xprev) / xprev) < 0.000001 Then Exit For
    If xnew <= min Then xnew = 0.5 * (min + xprev)
    If xnew >= max Then xnew = 0.5 * (max + xprev)
    xprev = xnew
   Next k:        x_i = xnew
  Case "GAMMA":  xprev = a1 * a2
   For k = 1 To 80
    CDF = .GammaDist(xprev, a1, a2, True):   pdf = .GammaDist(xprev, a1, a2, False)
    xnew = xprev - (CDF - .NormSDist(ni)) / pdf
    If Abs((xnew - xprev) / xprev) < 0.000001 Then Exit For
    If xnew <= 0 Then xnew = 0.5 * xprev
    xprev = xnew
   Next k:         x_i = xnew
  Case "PERTDIST":    mean = (a1 + 4 * a2 + a3) / 6:  xprev = mean:   min = a1:  max = a3
   If a2 = mean Then f = 6 Else f = (2 * a2 - a1 - a3) / (a2 - mean)
   a1 = (mean - min) * f / (max - min):  a2 = a1 * (max - mean) / (mean - min)
   GoTo 8
 End Select:  End With
End Function
```

Iterate for the inverse of beta dist.

Refinement

Iterate for the inverse of gamma distribution

Refinement

PERT distribution is a special case of Beta distribution, hence GoTo 8.

Fig. 8. Excel VBA code for the inverse $x_i = F^{-1}[\Phi(n_i)]$. Closed form solutions for the first eight distribution types (Normal, Lognormal, ..., Weibull), and refined Newton method for the other three distributions (BetaDist, Gamma, and PertDist)

range (a_2, a_3), the cumulative distribution function $F(x)$ – in which $\lambda = 1/\text{mean}$ – is set equal to the standard normal cumulative distribution $\Phi(n)$, followed by rearrangement:

$$F(x) = \frac{(e^{-\lambda a_2} - e^{-\lambda x})}{e^{-\lambda a_2} - e^{-\lambda a_3}} = \Phi(n), \tag{12a}$$

from which one obtains:

$$x = -\frac{1}{\lambda}\ln[e^{-\lambda a_2} - (e^{-\lambda a_2} - e^{-\lambda a_3})\Phi(n)] \tag{12b}$$

Equation (12b) has been coded in the two lines under Case "TR_EXP" in Fig. 8.

For beta, gamma, and PERT distributions, the Newton-Raphson (or Newton) iteration method is used to determine x such that $F(x) = \Phi(n)$:

$$x_{k+1} = x_k - \frac{F(x_k) - \Phi(n)}{\frac{d}{dx}[F(x_k) - \Phi(n)]} = x_k - \frac{F(x_k) - \Phi(n)}{f(x_k)} \tag{13}$$

where $F(x)$ is cumulative distribution and $f(x)$ is probability density function. The initial value prior to iterative looping by the Newton method is the mean value of the nonnormal distribution. This initial value is the ''xprev'' defined just prior to the For-Next looping, under cases BETADIST, GAMMA and PERTDIST in Fig. 8. The Newton method (Eq. (13)) code is indicated by the arrow under Cases BETADIST and GAMMA. The following statements (two lines below the arrowed Newton-method code) refine the Newton method by restricting the trial x values to within the lower and upper bounds (min and max, respectively):

For Case BETADIST: If xnew <= min Then xnew = 0.5* (min + xprev)
If xnew >= max Then xnew = 0.5* (max + xprev)
For Case GAMMA: If xnew <= 0 Then xnew = 0.5* xprev

The program Function x_i is called in cells G6:G10 of Fig. 6, by entering the formula '' = x_i(A6,C6:F6,M6)'' in cell G6, and autofilling down to cell G10. The arguments of Function x_i are *DistributionName*, *para* and n_i. In the fourth line of the program in Fig. 8, the *Select Case* control structure alters the flow of execution to one of several code segments, depending on the input of *DistributionName*. The third line ''With Application.WorksheetFunction'' enables liberal calls to Excel's built-in functions, using the syntax ''.NormSDist(·)'', ''.GammaDist(...)'', ''.BetaDist(...)'', ''.GammaLn'', where ''Application'' stands for Microsoft Excel. The use of these Excel objects (each a container of program codes) results in much simplicity, clarity, and brevity of the program codes and structure.

Low and Tang (2007) provides more details of the new method applied to the performance function $g(\underline{x}) = YZ - M$, a beam on elastic foundation, and a strut with complex supports.

In retrospect, the new approach of varying n_i evolves quite naturally from Eq. (3b), but would not have been suggested by the mathematically equivalent Eq. (3a). It is also not efficient to try to vary n_i and back-calculate x_i from $x_i = \mu_i^N + n_i\sigma_i^N$, because this leads to a recursive relationship since μ_i^N and σ_i^N are themselves intricate functions (Eqs. (4) and (5)) of x_i. The method illustrated in Fig. 6 succeeds by eliminating this recursive relationship, as μ_i^N and σ_i^N no longer appear in Eq. (9).

5. Ease of Initializing and Randomizing Dimensionless n_i Values in the New Method

As illustrated in Fig. 6, the new method varies the dimensionless numbers n_i, using Excel's built-in Solver for constrained optimization of Eq. (9); the basic random variables x_i are computed automatically from n_i either from closed form equations or via the refined Newton method iterations, as coded in Fig. 8, and constrained by the Excel Solver to be on the limit state surface; the means and standard deviations of equivalent normal distributions are not computed.

One major advantage of the new approach is that the initial n_i values in cells M6:M10 of Fig. 6, prior to Solver's constrained optimization, are zeros, which are straightforward to input. In contrast, the initial values of x_i in cells G6:G10 of Fig. 3 are the mean values $(35, 10, 15.3, 0.5, 0.08)$ of the basic nonnormal random variables. These mean values sometimes require separate calculations, for example when triangular, Weibull, gamma, beta or PERT distributions are involved, as explained in Fig. 3 of Low and Tang (2004).

Occasionally one may want to randomize the initial values of n_i (Fig. 6) or x_i (Fig. 3) prior to implementing the Solver optimization, to test whether the same design point and reliability index are obtained despite the randomized initial values. Randomizing n_i is done easily by invoking Excel\Tools\Data Analysis\Random Number Generation\ to generate five random numbers of a standard normal random variate $\mathrm{N}(0, 1)$, or $\mathrm{N}(0, 2)$, at one go in the $\mathrm{n_i}$ cells in Fig. 6, regardless of the type of nonnormal distributions of the original basic random variables. (Other distributions, e.g. uniform, can also be used for randomizing the initial values of n_i). In contrast, randomizing the initial values of x_i in Fig. 3 is less straightforward.

To illustrate, for the case in Fig. 6, ten sets of 5 numbers each were generated randomly in cells M6:M10 based on a uniform distribution with range $(-3, 3)$, each followed by Excel Solver optimization. The 10 values of the reliability index (cell H13) were identical as displayed, namely 1.557. Next, ten sets each were generated based on normal distribution (μ, σ) of $\mathrm{N}(0, 2)$ and $\mathrm{N}(0, 5)$, respectively. The 20 values of reliability index obtained by the Excel Solver were also identical as displayed $(= 1.557)$. This shows the robustness of the new approach based on the closed form inverse distribution and refined Newton method, for the case at hand with truncated exponential distributions of $\mathrm{i_w}$ and α, and 4-parameter general beta distributions of ϕ, c and b.

6. Effects of Correlations on the Required Reinforcing Force for a Target Reliability Index

If all random variables are uncorrelated (as implied in the correlation matrices of Figs. 3 and 6 in which diagonal entries are 1.0 and non-diagonal entries are all 0.0), the quadratic forms under the square root sign of Eqs. (3) and (9) reduce to $\sum(x_i - \mu_i^N)^2/\sigma_i^{N^2}$ and $\sum n_i^2$, respectively. The clarity and efficiency of the present ellipsoid-constrained-optimization approach – relative to the classical approach that requires orthogonalization of the correlation matrix – are more obvious when correlation exists for at least some of the random variables. It is generally known that the cohesion c and friction angle ϕ are likely to be negatively correlated – i.e., cohesive strength generally drops as the friction angle rises and vice versa. This section investigates the effect of negative correlation between c and ϕ on the reinforcing force T required to achieve a target reliability index of 2.5.

In addition, if the water which would fill the tension crack in a slope comes from direct surface run-off during heavy rains, one may reason that shallower crack depths tend to be water-filled more readily than deeper crack depths. This means that the tension crack depth z and $\mathrm{i_w}$ $(=\mathrm{z_w}/\mathrm{z})$ are likely to be negatively correlated, which in turn implies b and $\mathrm{i_w}$ are positively correlated because of the geometrical relationship

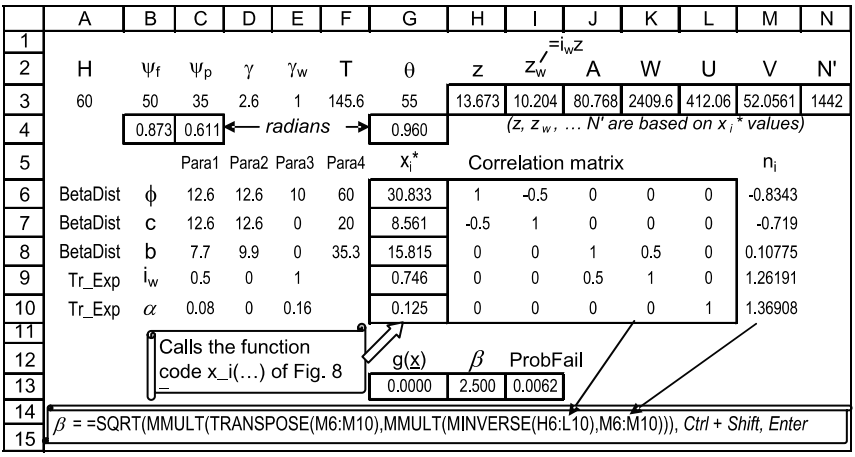

(a)

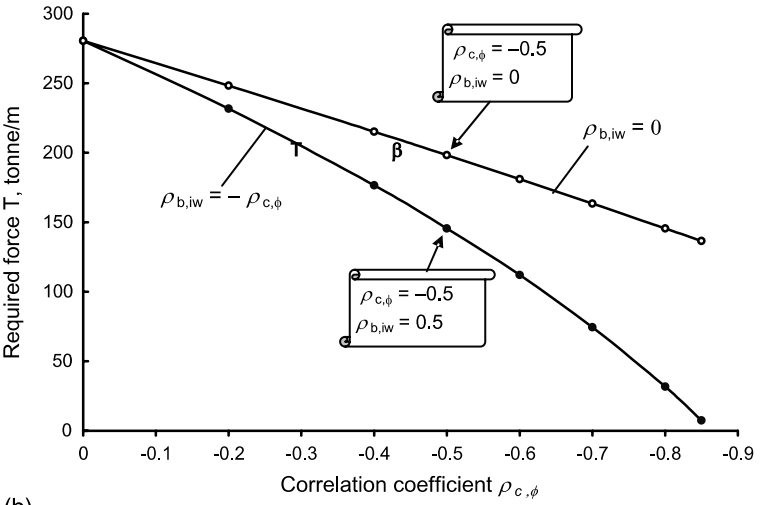

(b)

Fig. 9. Relation between required horizontal reinforcing force T and correlation coefficients, for a target reliability index of 2.5: (a) required T is 146 t/m when $\rho_{c,\phi} = -0.5$ and $\rho_{b,iw} = 0.5$; (b) variation of required horizontal T with correlation coefficients $\rho_{c,\phi}$ and $\rho_{b,iw}$

between z and b given in Fig. 2. For simplicity and illustrative purposes, a negative correlation coefficient -0.5 will be assumed between c and ϕ, and a positive correlation coefficient 0.5 between b and i_w.

Figure 9a shows that the required horizontal (i.e. $\theta = 55°$) reinforcing force T for a target reliability index of 2.5 is about 146 t/m, when c and ϕ are negatively correlated, with correlation coefficient $\rho_{c,\phi} = -0.5$, and b and i_w positively correlated, with $\rho_{b,i_w} = 0.5$. Note that the design point values of the resistance parameters ϕ and c, at 30.83° and 8.56 t/m^2, respectively (cells G6 and G7), are lower than their mean

values of 35° and 10 t/m^2 respectively. The design point values of the load parameters i_w and α, at 0.746 and 0.125, are above their respective mean values of 0.5 and 0.08. The analysis in Figs. 3 and 6, for uncorrelated random variables, is instructive in confirming that parameters with negative n_x or n_i values (cells O6:O8 in Fig. 3 and cells M6:M8 in Fig. 6) are resistance parameters, and parameters with positive n_x or n_i values (cells O9:O10 in Fig. 3 and cells M9:M10 in Fig. 6) are load parameters. In Fig. 9a, the above-mean value of 15.815 for width b (which acts as if it is a resistance parameter) is due to its positive correlation with i_w (a load parameter). This can be verified by performing a reliability analysis with 0 replacing the values 0.5 in cells K8 and J9. The reliability index β obtained is 2.29, and the design point values of ϕ, c, b, i_w and α are 32.04, 8.83, 12.81, 0.80 and 0.12, respectively, in which the design point value of b, at 12.81 m, is lower than its mean value of 15.3 m. (Taking partial derivatives of $g(\underline{x})$ or F_s with respect to b and z respectively will also verify that the role of width b is similar to a resistance parameter and that of vertical crack depth z is similar to a load parameter.)

Figure 9b shows that the horizontal reinforcing force T required to achieve a reliability index of 2.5 depends on the values of the correlation coefficients. The seven open-circle points defining the upper curve were obtained from reliability analyses using $\rho_{c,\phi}$ values (in cells I6 and H7) of -0.2, -0.4, -0.5, -0.6, -0.7, -0.8 and -0.85, respectively, while ρ_{b,i_w} values (in cells K8 and J9) were zeros. The seven solid-circle points defining the lower curve were obtained from reliability analyses using $\rho_{c,\phi}$ values (in cells I6 and H7) of -0.2, -0.4, -0.5, -0.6, -0.7, -0.8 and -0.85, respectively, and using ρ_{b,i_w} values (in cells K8 and J9) of 0.2, 0.4, 0.5, 0.6, 0.7, 0.8 and 0.85, respectively, so that $\rho_{b,i_w} = -\rho_{c,\phi}$ for each solid circle. The plots show that a smaller reinforcing force T is required to achieve a reliability index β of 2.50 when strength parameters c and ϕ are negatively correlated. As explained earlier, a positive correlation between width b and water-depth indicator i_w ($= z_w/z$) means a negative correlation between z and i_w. Since z and i_w are load parameters, one may conclude from the lower curve of Fig. 9b that negatively correlated load parameters will further reduce the reinforcing force T required for a target reliability index. Negatively correlated load parameters represent a more favorable scenario than uncorrelated or positively correlated load parameters, for this implies that unfavorable load combinations (i.e., both loads at high values) are less likely to occur. Similarly, negatively correlated strength parameters (c and ϕ) represent a more favorable scenario than uncorrelated or positively correlated strength parameters, because this implies that unfavorable strength combinations (both c and ϕ at low values) are less likely to occur than if the strength parameters are uncorrelated or positively correlated.

For each parameter, the ratio of the mean value to the x^* value (e.g. 35/30.833 for ϕ and 10/8.561 for c, for the case in Fig. 9) is similar in nature to the partial factors in limit state design (e.g., Eurocode 7). However, in a reliability-based design one does not specify the partial factors. The design point values (x^*) are determined automatically and reflect sensitivities, standard deviations, correlation structure, and probability distributions in a way that prescribed partial factors cannot reflect.

Figure 10 shows alternative perspectives of the effects of correlations on the required reinforcing force for a target reliability index of 2.50. In both the plots of Fig. 10, the first open-circle point closest to the y axis corresponds to $\rho_{c,\phi} = 0$ and

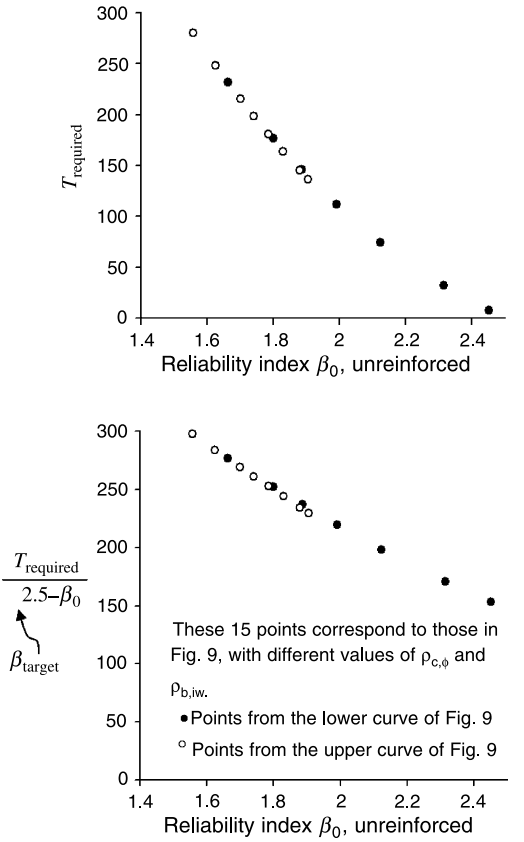

Fig. 10. Different perspectives of the two curves of Fig. 9. The lower plot shows the required T force per unit increase in reliability index; it is obtained from the upper plot by dividing the y values of the upper plot by $(\beta_{target} - \beta_0)$

$\rho_{b,iw} = 0$, with unreinforced $\beta_0 = 1.557$, as analyzed in Fig. 6. The right-most solid circle has $\rho_{c,\phi} = -0.85$ and $\rho_{b,iw} = 0.85$, with unreinforced $\beta_0 = 2.451$. These two cases require an increase in reliability index $(\Delta\beta = \beta_{target} - \beta_0)$ of 0.943 and 0.049, respectively. Hence the $T_{required}$ is much larger in the former than in the latter.

The reliability index of 2.50 in Fig. 9a corresponds to a probability of failure of 0.62% based on $P_f \approx \Phi(-\beta)$. For comparison, three Monte Carlo simulation with Latin Hypercube sampling (each of size 100,000) using @RISK software yielded P_f values of 0.37, 0.33, 0.31%, or an average of about 0.34%. The difference between 0.62% and 0.34% is due to the more approximate nature of FORM when truncated exponentials are involved.

Results from Monte Carlo simulations are more accurate when sufficient iterations are used. However, for reliability-based design like the case at hand, the reinforcing force T required to achieve a target reliability index of 2.5 is initially unknown. To get the required T for a target probability of failure one would need to try different T values – relatively fast when using the reliability index criterion of $\beta = 2.5$, but time-

consuming if based on Monte Carlo simulations for a target probability of failure of 0.62% say, because each trial value of T requires renewed simulation (each of sample size 100,000 or more). Since reliability-based design typically aims at a target reliability index greater than 2.5 (or 3.0), the estimated probability of failure is smaller than 0.6% (or 0.13%), from $P_f \approx \Phi(-\beta)$. Engineers have to decide whether for practical purposes it is adequate to go for reliability-based design in which the implied *small* probability of failure (based on $P_f \approx \Phi(-\beta)$) is approximate but similarly small as the theoretical probability of failure, or engage in trial and error design via multi-session Monte Carlo simulations. Prior comparative studies (as in this section) on a problem-domain-specific basis would be useful. The combined use of both FORM and Monte Carlo simulation methods is also a possibility. For instance, in the light of the comparison (0.62% vs. 0.34%) in the previous paragraph, suppose a probability of failure of 0.5% is the desired target for the case at hand, one may design the T force for a reliability index corresponding to a probability of failure of $(0.0062/0.0034) * 0.005$, i.e., $-\beta = \Phi^{-1}(P_f) = \text{normsinv}(0.0091)$, hence $\beta = 2.36$. For the set-up in Fig. 9, a few trial values of T using Solver led (within a minute) to the value T = 114 t/m for $\beta = 2.36$. To verify, three Monte Carlo simulations (with T = 114) using @RISK each with Latin Hypercube sampling size of 100,000 yielded probability of failure of 0.485, 0.481, and 0.512%, respectively; the average is practically the desired 0.5%.

7. Summary and Conclusions

A two-dimensional jointed rock slope in Hong Kong was analyzed probabilistically using a new Low and Tang (2007) algorithm that combines the inverse distribution functions and refined Newton method with Microsoft Excel's built-in constrained optimization routine. The new procedure (Eqs. (9) and (11b), and Figs. 6 and 8) obtains the same reliability index and design point as the classical first-order reliability method (FORM) for correlated nonnormals, but is more direct and transparent. The perspective of expanding dispersion ellipsoid in the original space of random variables was offered as a conceptual aid to understand intuitively the meaning of the reliability index and the design point. A major advantage of the new procedure is the ease with which the changing cells (cells M6:M10, Fig. 6) can be initialized and randomized.

Five parameters were treated as random variables in the Hong Kong slope. Three of them, namely cohesion c, friction angle ϕ, and horizontal distance b between crest and tension crack, were modeled using the versatile 4-parameter generalized beta distributions. The other two parameters, the water-depth indicator (i_w) of tension crack and earthquake acceleration coefficient α, were modeled by a truncated exponential distributions. The latter part of this paper further investigates the effects of negative correlation between c and ϕ and positive correlation between b and i_w on the reinforcing force required to achieve a target reliability index.

Reliability-based design can be done quickly and efficiently using the procedure presented in the paper. However, the probabilities of failure inferred from reliability indices were approximate for the Hong Kong slope, due to the use of two truncated exponentials. Monte Carlo simulation is robust and in principle accurate when the sample size is sufficiently large. It is suggested that reliability-based design can play a

useful complementary role to Monte Carlo simulations, particularly in reliability-based design where trial and error design via Monte Carlo simulation could be time-consuming. A simple strategy was proposed to harness the strengths of both the reliability-based design (with its efficiency) and the Monte Carlo simulation (with its robustness) so that reliability-based design can be accomplished with efficiency and accuracy.

The meaning of the computed reliability index and the inferred probability of failure is only as good as the analytical model and the statistical inputs underlying the performance function. The ''probability of failure'' – from reliability index or from Monte Carlo simulations – should be regarded more restrictively as *the probability that the performance function $g(x)$ will yield unacceptable values for the analytical and statistical models adopted*. Nevertheless, even this restrictive sense of reliability index (and the corresponding probability of failure) is more useful than the lumped factor of safety approach or the partial factors approach, both of which are also only as good as their underlying analytical models.

The new method presented in this study operates in the ubiquitous spreadsheet platform; it obtains the same reliability index and design point as the classical FORM, but is operationally more intuitive and transparent than the latter. The new method does not involve complicated transformation, and can therefore play a useful complementary role to the classical FORM approach. If information pertaining to the independent set of transformed standard normal variates (of the classical FORM) is desired, such transformation can be done after the design point has been obtained efficiently by the method presented herein.

References

Ang, H. S., Tang, W. H. (1984): Probability concepts in engineering planning and design, Vol. 2. Decision, risk, and reliability. John Wiley, New York.

Baecher, G. B., Christian, J. T. (2003): Reliability and statistics in geotechnical engineering. Chichester, West Sussex, England; J. Wiley, Hoboken, NJ

Chen, X., Lind, N. C. (1983): Fast probability integration by three-parameter normal tail approximations. Struct. Saf. 1(4), 269–276.

Der Kiureghian, A., Liu, P. L. (1986): Structural reliability under incomplete probability information. J. Eng. Mech. ASCE 112(1), 85–104.

Der Kiureghian, A., Lin, H. Z., Hwang, S. J. (1987): Second-order reliability approximations. J. Eng. Mech. ASCE 113(8), 1208–1225.

Ditlevsen, O. (1981): Uncertainty modeling: with applications to multidimensional civil engineering systems. McGraw-Hill, New York.

Haldar, A., Mahadevan, S. (1999): Probability, reliability and statistical methods in engineering design. John Wiley, New York.

Hasofer, A. M., Lind, N. C. (1974): Exact and invariant second-moment code format. J. Eng. Mech. ASCE, New York 100, 111–121.

Hoek, E. (2006): Practical rock engineering. Chapter 7: A slope stability problem in Hong Kong; and Chapter 8: Factor or safety and probability of failure. In: http://www.rocscience.com/hoek/PracticalRockEngineering.asp.

Low, B. K., Tang, W. H. (1997a): Efficient reliability evaluation using spreadsheet. J. Eng. Mech. ASCE, New York 123(7), 749–752.

Low, B. K., Tang, W. H. (1997b): Reliability analysis of reinforced embankments on soft ground. Can. Geotech. J. 34(5), 672–685.

Low, B. K., Tang, W. H. (2004): Reliability analysis using object-oriented constrained optimization. Struct. Saf. 26(1), 69–89 (An Excel file for hands-on is downloadable from http://alum.mit.edu/www/bklow).

Low, B. K. (2005): Reliability-based design applied to retaining walls. Geotechnique 55(1), 63–75.

Low, B. K. (2007): Reliability analysis of rock slopes involving correlated nonnormals. Int. J. Rock Mech. Min. Sci. 44(6), 922–935.

Low, B. K., Tang, W. H. (2007): Efficient spreadsheet algorithm for first-order reliability method. J. Engrg. Mechanics ASCE (Accepted).

Melchers, R. E. (1999): Structural reliability analysis and prediction, 2nd ed. Appendix B2. New York: John Wiley.

Rackwitz, R., Fiessler, B. (1978): Structural reliability under combined random load sequences. Comput. Struct. 9(5), 484–494.

Rackwitz, R. (2001): Reliability analysis – a review and some perspectives. Struct. Saf. 23(4), 365–395.

Shinozuka, M. (1983): Basic analysis of structural safety. J. Struct. Eng. ASCE 109(3), 721–740.

Veneziano, D. (1974): Contributions to second moment reliability. Research Report No. R74-33. Department of Civil Engng., MIT, Cambridge, Masachusetts.

Wu, Y. T., Wirsching, P. H. (1987): New algorithm for structural reliability estimation. J. Eng. Mech. ASCE 113(9), 1319–1335.

Zhao, Yan-Gang, Tetsuro Ono (2001): Moment methods for structural reliability. Struct. Saf. 23(1), 47–75.

Author's address: Dr. Bak Kong Low, School of Civil and Environmental Engineering, Nanyang Technological University, Block N1 #1b-40, 50 Nanyang Avenue, 639798 Singapore; e-mail: bklow@alum.mit.edu